First-principles prediction of the thermodynamic stability of xenon in monoclinic, tetragonal, and yttrium-stabilized cubic ZrO_{2}

Chao Jiang, Xiang-Yang Liu, and Kurt E. Sickafus

Phys. Rev. B **83**, 052103 — Published 28 February 2011

DOI: 10.1103/PhysRevB.83.052103

First-principles prediction of the thermodynamic stability of xenon in monoclinic, tetragonal, and yttrium stabilized cubic ZrO_2

Chao Jiang[1]*, Xiang-Yang Liu[2]*, and Kurt E. Sickafus[2]

[1]State Key Laboratory of Powder Metallurgy, Central South University, Changsha, Hunan 410083, P. R. China

[2]Materials Science and Technology Division, Los Alamos National Laboratory, Los Alamos, NM 87545, USA

Abstract

Fission product incorporation in ceramic fuels has long been an active area of research. In this work, we consider a special case of xenon incorporation in ZrO_2 in the framework of closed systems under extreme radiation conditions where thermal defects are less important than cascade driven defects. The energetics of a variety of defect configurations associated with xenon incorporation are considered. We use first-principles density functional theory (DFT) calculations to predict the thermodynamic stability of xenon in different ZrO_2 structural forms, including monoclinic, tetragonal, and yttrium stabilized cubic ZrO_2. Two defect configurations are found to dominate the fission gas incorporation process: xenon interstitial and oxygen substitutional configurations. In yttrium stabilized cubic ZrO_2, the pre-existing structural oxygen vacancies provide ideal sites for Xe incorporation since no oxygen Frenkel pairs need to be formed. The charge transfer issue in oxides modeling is important in defects calculations. This issue has also been addressed through our supercell benchmark calculations.

Keywords: DFT; Point defects; Oxide ceramic; Radiation effect

Corresponding authors: xyliu@lanl.gov (XY Liu) and chaopsu@gmail.com (C Jiang)

Fission product incorporation in fluorite-structured oxides (such as UO_2) has long been an active area of research. Understanding of fission products (FP) at the microscopic level is important in terms of understanding the fuel system at a macroscopic level. Additionally, understanding of fission products in general type oxide ceramics yields scientific knowledge on the mutual interactions of fission products and associated defects, which may help to design better ceramic fuel forms [1]. Our previous modeling studies on fission products in oxides include MgO, HfO_2, CeO_2, and UO_2 [2-4]. Here, we report on fission product behavior in various polymorphs of zirconia (ZrO_2). Zirconia has long been considered a potential candidate for a non-fertile, *inert matrix* nuclear fuel material (see, e.g., Ref. [5]), mainly due to its exceptional radiation tolerance of this oxide [6].

In the standard theoretical approach, the energetics of fission product incorporation are investigated by assuming that those FP occupy pre-existing intrinsic trap sites (e.g., mono-vacancies, di-vacancies, and Schottky defects) that are thermally generated under thermodynamic equilibrium. Conventionally, the incorporation energy is defined as the energy required to bring a fission product from infinity and place it at a pre-existing trap site [7]:

$$E^{inc} = E_{total} - E_{trap} - E_i \quad (1)$$

where E_{total} is the total energy of the system with fission product incorporated at a particular defect site. E_{trap} is the total energy of the cell with a particular defect, but without the fission product. E_i is the energy of a single isolated fission product. As has been pointed out by Nerikar et al. [3], Eq. (1) assumes that there are always abundant traps sites available for fission product incorporation and thus does not account for the energy needed to form the trap sites themselves. Consequently, it is valid only when the concentrations of FP are comparable to those of pre-existing trap sites. In nuclear fuels that are exposed to extreme radiation environments, however,

the concentrations of fission products will far exceed those of the thermally generated trap sites, and therefore those "trap-sites" have to be forced to form in a non-equilibrium manner, mostly due to the generation of cation and anion Frenkel pairs (i.e., simultaneous generation of a vacancy and an interstitial atom) during cascade events. Furthermore, as Frenkel pairs are created, the migration of interstitials to surfaces or grain boundaries can be kinetically difficult, especially in coarse-grained materials. Under such circumstances, it may be more appropriate to consider a closed system (i.e., all interstitials from the cascade generated Frenkel pairs are assumed to remain in the material) when determining the most favorable location of FP in an irradiated material.

In this study, we apply our closed-system concept to examine xenon (Xe) fission gas incorporation in ZrO_2 polymorph oxides under non-equilibrium defect conditions. ZrO_2 polymorph studied includes monoclinic (space group $P2_1/c$), tetragonal ($P4_2/nmc$), and yttrium stabilized cubic ZrO_2 ($Fm\bar{3}m$). Regular DFT techniques can be applied perfectly well to ZrO_2 oxide system. This is in comparison to the actinide UO_2 oxide system, which requires DFT+*U* or hybrid functional treatment due to its strong correlated and localized 5*f* electrons. In such treatment, additional complicated issue such as metastable electronic/magnetic states may possibly happen [8]. In the study of ZrO_2 oxide system, however, such issue needs not to be considered, thus a simpler picture may be drawn from our calculations. The results from our study may also be a useful benchmark providing insights to the more complicated UO_2 system.

We obtain the energetics of Xe incorporation in ZrO_2 using a first-principles supercell approach [9, 10]. Large-sized supercells are employed in our study in order to avoid the unphysical (elastic and electrostatic) interactions between a defect and its periodic images. For pure monoclinic and tetragonal ZrO_2, we construct a 324-atom 3×3×3 supercell based on the

original 12-atom monoclinic (tetragonal) unit cell. To model the yttrium stabilized cubic ZrO_2, we create a 96-atom 2×2×2 supercell of fluorite ZrO_2 and randomly replace 8 of its 32 Zr atoms (corresponding to a 25% doping level) with Y atoms. To maintain charge neutrality within the supercell, we then randomly remove 4 of the 64 O atoms, thus creating 4 structural oxygen vacancies. First-principles total energy calculations are performed using projector augmented wave (PAW) [11] pseudopotentials within the generalized gradient approximation (PW91-GGA) [12], as implemented in Vienna *ab initio* simulation package (VASP) [13]. For computational efficiency, the 4*s* and 4*p* electrons of Zr are kept frozen in the core. As shown in Table 1, our choice of pseudopotentials can give structural properties and relative energies of three pure ZrO_2 polymorphs in reasonably good agreement with experiments [14, 15]. A plane-wave cutoff energy of 250 eV is used throughout our calculations. The *k*-point meshes for Brillouin zone sampling are constructed using the Monkhorst–Pack scheme [16] and care has been taken to ensure convergence with respect to *k*-points. According to our convergence tests, a 1×1×1 and a 2×2×2 *k*-point mesh are found to be sufficient for the 324- and 96-atom supercells, respectively. During structural relaxations, the lattice vectors of the supercells are kept frozen while all atom positions within a supercell are allowed to relax until the Hellmann-Feynman forces acting on the atoms are less than 0.05 eV/Å. Further relaxations of unit cell volumes have only negligible effects on our final results.

In the case of Xe incorporation in pure monoclinic and tetragonal ZrO_2, we define the incorporation energy in a closed system as follows:

$$E_{closed}^{inc} = E[Zr_{N-x}O_{2N-y}Xe] + xE[Zr_NO_{2N}Zr] + yE[Zr_NO_{2N}O] - (1+x+y)E[Zr_NO_{2N}] - E[Xe] \quad (2)$$

where $E[Zr_{N-x}O_{2N-y}Xe]$ is the total energy of a supercell in which a single Xe atom occupies a trap site formed by x Zr vacancies and y O vacancies, expelling x Zr and y O atoms into

interstitial positions. Note that, instead of displacing existing Zr or O atoms, Xe atoms can also choose to go directly into an empty interstitial position. In such a case, we have x=0 and y=0. $E[Zr_N O_{2N} Zr]$ and $E[Zr_N O_{2N} O]$ are the total energies of a supercell containing a single Zr or O interstitial atom, respectively. $E[Zr_N O_{2N}]$ denotes the total energy of a perfect ZrO_2 lattice. $E[Xe]$ is the energy of isolated Xe, calculated using a 10Å×10Å×10Å supercell with a single Xe atom placed at its center. It is worth pointing out here that, our concept of E^{inc}_{closed} is fundamentally different from the concept of solution energy proposed by Grimes et al. [7], which is defined as the sum of E^{inc} and the trap site formation energy. We assume that, as Frenkel pairs are created, the migration of interstitial atoms to surfaces or grain boundaries is kinetically hindered, and those interstitial atoms thus always stay within the system. In contrast, Grimes et al. [7] assume that those interstitial atoms can be rapidly annihilated at surfaces or grain boundaries. Presumably, our concept of incorporation energy in a closed system is more applicable to coarse-grained materials, while the concept of solution energy may be more relevant to nano-sized materials.

We consider Xe incorporation at the interstitial site, O vacancy, Zr vacancy, O di-vacancy, and a di-vacancy consisting of a Zr vacancy and an O vacancy in close proximity. The most likely interstitial sites (i.e., the largest interstices) in monoclinic and tetragonal ZrO_2 are identified using the computational method developed in our previous study [17], and are graphically shown in Fig. 1. In modeling oxides, proper treatment of charged defects and the associated charge transfer is an important issue. In this work, we adopt the full charge compensation model, i.e., we assume that all defects are in their most probable ionic charge states, as defined by their charge states in perfect bulk. We model oxygen interstitial as O_i^{-2} and Zr interstitial as Zr_i^{+4}. When a Xe atom occupies a trap site consisting of x O vacancies and y Zr

vacancies, it is assumed to carry a charge of q=2x-4y. When a Xe atom occupies an interstitial site, it is assumed to be charge neutral (q=0). In order to simulate charged defects, we artificially add or subtract electrons from a defect-containing supercell. All the charges are then automatically compensated by a neutralizing jellium background charge in VASP. We also apply the monopole correction to the charged system. The details of charged system treatment were discussed in our previous study [2] and are not repeated here.

Our final calculated closed-system incorporation energies E_{closed}^{inc} of Xe in pure tetragonal and monoclinic ZrO_2 are summarized in Table 2. In tetragonal ZrO_2, it is energetically most favorable for Xe to occupy an oxygen position, expelling the original oxygen atom to an interstitial position. In comparison, while Zr vacancies and di-vacancies (O+O and O+Zr) will provide a larger space for Xe incorporation, they are not favorable trap sites for Xe due to the energy penalty associated with the creation of interstitial atoms. In monoclinic ZrO_2, there exist two different types of oxygen sites: O3 site is threefold coordinated by Zr while O4 site is fourfold coordinated by Zr. It can be seen that O3 vacancy provides a better site for Xe incorporation compared with O4 vacancy. This can be understood since O3 site is coordinated by only three Zr atoms and is therefore more open than O4 site, as has also been pointed out by Foster et al. [9, 18]. Interestingly, instead of occupying an O site, Xe prefers to directly occupy an interstitial position in monoclinic ZrO_2. Presumably, this is due to the lower packing density (and thus more empty space) of monoclinic ZrO_2 than that of tetragonal ZrO_2 (see Table 1).

For the sake of completeness, we have also computed the conventional incorporation energies (E^{inc}) of Xe by rewriting Eq. (1) as follows:

$$E^{inc} = E[Zr_{N-x}O_{2N-y}Xe] - E[Zr_{N-x}O_{2N-y}] - E[Xe] \quad (3)$$

where $E[Zr_{N-x}O_{2N-y}]$ is the total energy of a supercell containing x Zr vacancies and y O

vacancies in close proximity. From Table 2, a clear trend can be seen that E^{inc} monotonically decreases with increasing size of the trap site, suggesting the Xe is more stable in larger trap site (for instances, a di-vacancy is a better trap site than a mono-vacancy, and a Zr vacancy is a more favorable incorporation site than O vacancy). Note that this is however not the case when judging from our closed-system incorporation energies, for reasons already discussed above.

In a few cases, we have also performed additional calculations assuming all defects to be charge neutral. Interestingly, after full structural relaxations, we find that a neutral O interstitial in monoclinic ZrO_2 forms strong covalent bonding with a lattice oxygen atom, forming a dumbbell configuration (see Fig. 2). In contrast, a doubly charged O interstitial instead occupies a new triple site in monoclinic ZrO_2. Such results are fully-consistent with the previous studies by Foster et al. [9] and Zheng et al. [10]. From Table 2, it can be seen that neutral calculations are clearly physically unrealistic since they yield incorporation energies that are too high. This is a clear indication that the charge transfer issue has to be correctly accounted for in order to obtain correct energetics. In reality, the defects can also adopt charges other than the ones assumed in our study (e.g., O_i^0, O_i^{-1}, and Zr_i^{+3}). To validate our adoption of the full charge compensation model, we have additionally created a 324-atom 3×3×3 supercell of tetragonal ZrO_2 and replaced one of its O atoms with Xe. To make the system a closed one, we then reinsert one O atom back into the supercell at an interstitial site. Here the O interstitial and Xe_O defects are widely separated in the supercell. Since both Xe_O and O_i defects are now contained in the *same* supercell, there is no need to specify their individual charge states in the supercell calculations. The incorporation energy of Xe at an O vacancy in pure tetragonal ZrO_2 can then be directly obtained as the total energy difference between such a supercell and a perfect tetragonal ZrO_2 supercell, minus the energy of an isolated Xe atom. The final value is calculated to be

14.16 eV, which is in excellent agreement with the result obtained from Eq. (2) (14.37 eV). Our supercell benchmark calculations thus unambiguously support our assumptions regarding the charge states of defects.

Fig. 3 shows the crystal structure model of yttrium stabilized cubic ZrO_2 adopted in our study. Unlike pure ZrO_2, the four existing structural oxygen vacancies in Y-stabilized cubic ZrO_2 already provide ideal sites for Xe incorporation. Unlike the thermally generated vacancies, those structural vacancies are abundant and are stable even at $T = 0$ K. As a consequence, a fission product such as Xe atom can directly occupy a structural oxygen vacancy without the need to form an oxygen Frenkel pair. In such a case, the conventional (E^{inc}) and closed-system (E^{inc}_{closed}) definitions of incorporation energies become identical. As shown in Table 2, the incorporation energy of Xe in Y-stabilized ZrO_2 is significantly smaller than those of pure monoclinic and tetragonal ZrO_2. The present results thus indicate that oxides with structural vacancies have much larger tendencies to accommodate fission products than pure ones.

To summarize, we propose a closed-system concept to predict the most favorable location of Xe in three ZrO_2 structural forms: monoclinic, tetragonal, and yttrium stabilized cubic ZrO_2. While the conventional definition of FP incorporation energy remains valid at very small FP concentrations, our closed-system concept is more applicable when FP concentrations far exceed those of the thermally generated trap sites and when the annihilation of cascade driven interstitials is kinetically difficult. By performing first-principles calculations on large-sized supercells, we find that two defect configurations seem to dominate the fission gas incorporation process due to their low energies: xenon interstitial and oxygen substitutional configurations. This is in contrast to the currently accepted view that Xe is most stable in the largest trap site.

We believe that our proposed closed-system concept may be important for understanding fission gas behavior in nuclear fuels under extreme irradiation conditions.

We acknowledge helpful discussions with Blas Uberuaga and Steve Valone. This work is supported by the Los Alamos National Laboratory (LANL) Directed Research and Development Program. LANL is operated by Los Alamos National Security, LLC, for the National Nuclear Security Administration of the U.S. Department of Energy under Contract No. DE-AC52-06NA25396.

References

[1] M. Barrachin, R. Dubourg, M. P. Kissane, and V. Ozrin, J. Nucl. Mater. **385**, 372 (2009).

[2] X.-Y. Liu, B. P. Uberuaga and K. E. Sickafus, J. of Phys.: Condensed Matter **21**, 045403 (2009).

[3] P. V. Nerikar, X.-Y. Liu, B. P. Uberuaga, C. R. Stanek, S. R. Phillpot, and S. B. Sinnott, J. of Phys.: Condensed Matter **21**, 435602 (2009).

[4] X.-Y. Liu, B. P. Uberuaga, P. V. Nerikar, C. R. Stanek, and K. E. Sickafus, Nucl. Instr. and Meth. B **268**, 3014 (2010).

[5] K. E. Sickafus, R. J. Hanrahan, Jr., K. J. McClellan, J. N. Mitchell, C. J. Wetteland, D. P. Butt, P. Chodak, III, K. B. Ramsey, H. T. Blair, K. Chidester, H. Matzke, K. Yasuda, R. A. Verrall and N. Yu, Ceram. Bull. **78 (1)**, 69 (1999).

[6] K. E. Sickafus, H. Matzke, T. Hartmann, K. Yasuda, J. A. Valdez, P. Chodak, III, M. Nastasi and R. A. Verrall, J. Nucl. Mater. **274**, 66 (1999).

[7] R. W. Grimes and C. R. A. Catlow, Phil. Trans. R. Soc. A **335**, 609 (1991).

[8] B. Dorado, B. Amadon, M. Freyss, M. Bertolus, Phys. Rev. B **79**, 235125 (2009).

[9] A. S. Foster, V. B. Sulimov, F. Lopez Gejo, A. L. Shluger, and R. M. Nieminen, Phys. Rev. B **64**, 224108 (2001).

[10] J. X. Zheng, G. Ceder, T. Maxisch, W. K. Chim, and W. K. Choi, Phys. Rev. B **75**, 104112 (2007).

[11] G. Kresse, D. Joubert, Phys. Rev. B **59**, 1758 (1999).

[12] J. P. Perdew, J. A. Chevary, S. H. Vosko, K. A. Jackson, M. R. Pederson, D. J. Singh, and C. Fiolhais, Phys. Rev. B **46**, 6671 (1992).

[13] G. Kresse and J. Furthmuller, Phys. Rev. B **54**, 11169 (1996).

[14] P. Aldebert and J. P. Traverse, J. Am. Ceram. Soc. **68**, 34 (1985).

[15] C. J. Howard, R. J. Hill, and B. E. Reichert, Acta Crystallogr. Sect. B: Struct. Sci. **44**, 116 (1988).

[16] H. J. Monkhorst, J. D. Pack, Phys. Rev. B **13**, 5188 (1972).

[17] C. Jiang, S. A. Maloy, and S. G. Srinivasan, Scripta Mater **58**, 739 (2008).

[18] A. S. Foster, A. L. Shluger, and R. M. Nieminen, Phys. Rev. Lett. **89**, 225901 (2002).

Table 1. First-principles calculated structural parameters for ZrO_2 in monoclinic, tetragonal, and cubic crystal structures. Experimental data from Refs. [14] and [15] are also shown in parentheses. The relative energies between difference phases of ZrO_2 are also given.

Structure	*a*(Å)	*B*(Å)	*c*(Å)	*β*(°)	Volume (Å^3/f.u.)	ΔE (eV/f.u.)[a]
Monoclinic	5.09 (5.15)	5.25 (5.21)	5.22 (5.31)	98.8 (99.2)	34.5 (35.22)	-0.16 (-0.12)
Tetragonal	3.59 (3.57)	-	5.13 (5.18)	90	33.02 (34.07)	-0.05 (-0.06)
Cubic	5.07 (5.09)	-	-	90	32.55 (32.97)	0

[a]Using the cubic phase as the reference state.

Table 2. Closed-system and conventional incorporation energies, E_{closed}^{inc} and E^{inc}, of Xe in monoclinic, tetragonal, and Y_2O_3-stabilized cubic ZrO_2. For tetragonal and monoclinic ZrO_2, we have also performed a few neutral calculations, and such results are shown in parentheses for the sake of comparison.

Structure	Trap site	Incorporation energy (eV)	
		E_{closed}^{inc}	E^{inc}
Pure Monoclinic ZrO_2	Interstitial	11.21	-
	O3 vacancy	11.94 (15.70)	6.90
	O4 vacancy	13.95 (17.71)	8.21
	Zr vacancy	17.46	6.01
Pure Tetragonal ZrO_2	Interstitial	15.02	-
	O vacancy	14.37 (20.93)	10.26
	Zr vacancy	18.73	7.79
	O vacancy+Zr vacancy	17.79	4.26
	O vacancy+O vacancy	17.50	7.83
Cubic Y_2O_3-stabilized ZrO_2	O structural vacancy 1	8.56	-
	O structural vacancy 2	7.74	-
	O structural vacancy 3	7.83	-
	O structural vacancy 4	8.00	-

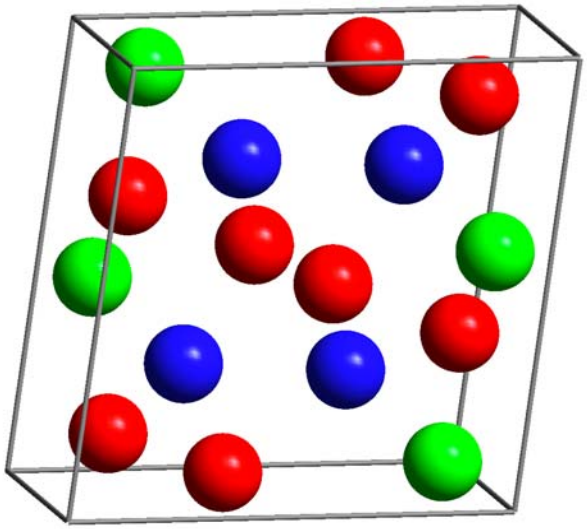

(a) Monoclinic

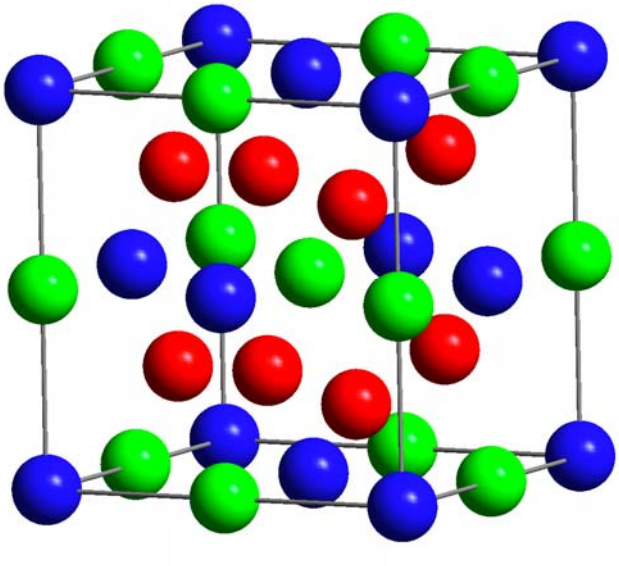

(b) Tetragonal

Fig. 1. Interstitial sites in monoclinic (a) and tetragonal (b) ZrO_2 considered in the present study. Blue and red spheres represent Zr and O atoms, respectively. Green spheres indicate the positions of the interstitial sites, which are all symmetrically equivalent.

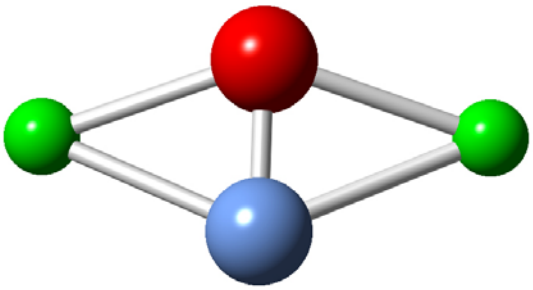

(a) Neutral oxygen interstitial

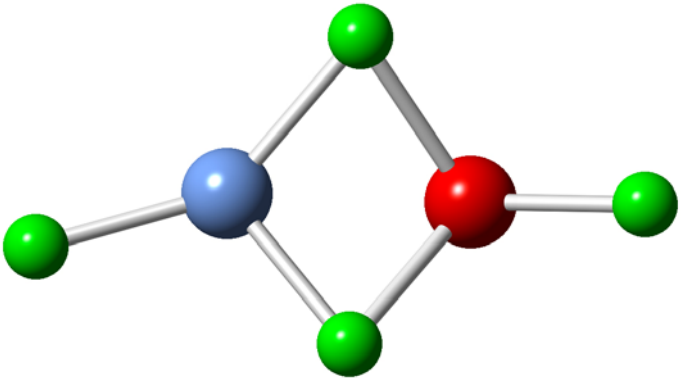

(b) Doubly-charged oxygen interstitial

Fig. 2. Illustration of the relaxed geometry of neutral and doubly-charged oxygen interstitial atoms in pure monoclinic ZrO_2. Green spheres represent Zr atoms, red spheres represent oxygen atoms, and blue spheres denote interstitial oxygen atoms.

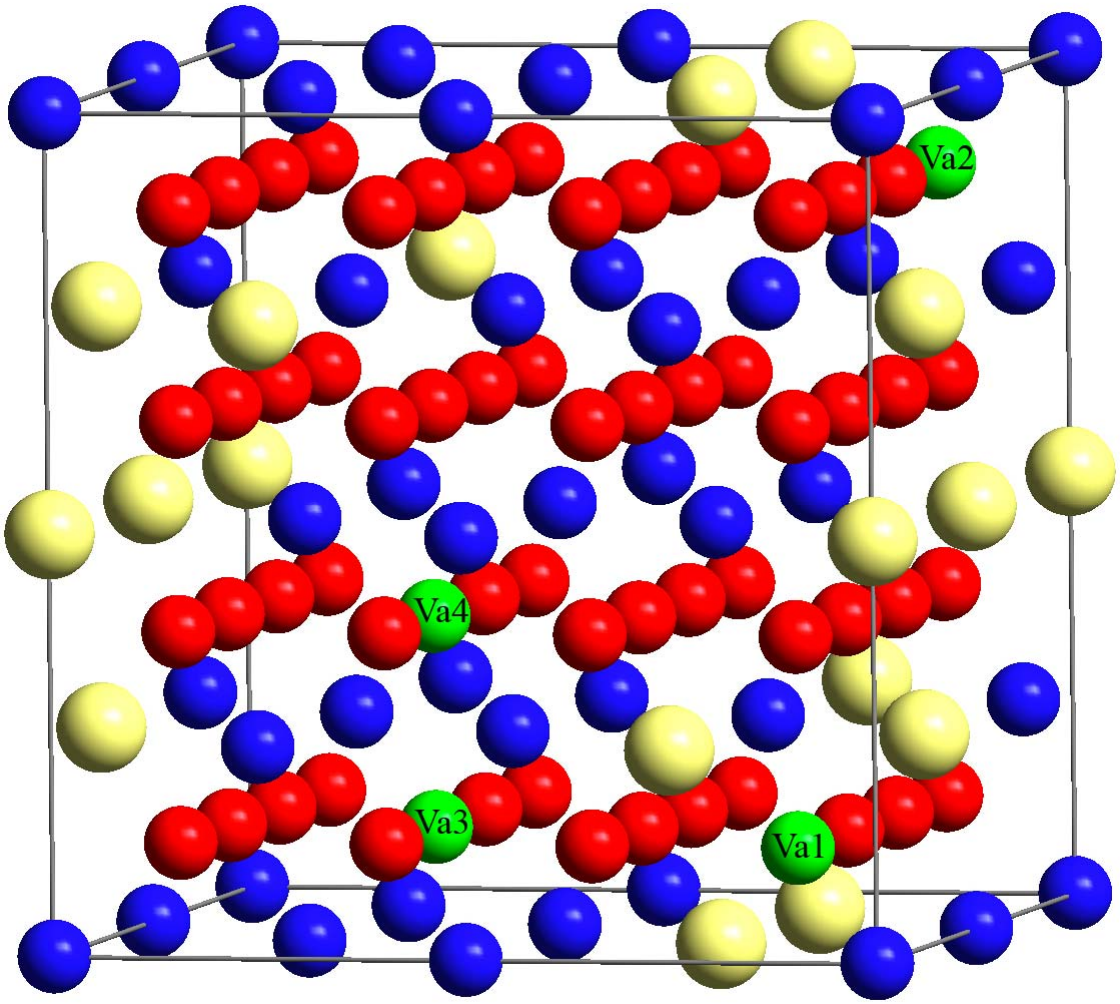

Fig. 3. Structural model for Y_2O_3-stabilized cubic ZrO_2. Blue, yellow and red spheres represent Zr, Y and O atoms, respectively. Green spheres indicate the positions of the structural oxygen vacancies.